

Crystallization Kinetics of Concurrent Liquid–Metastable and Metastable–Stable Transitions, and Ostwald’s Step Rule

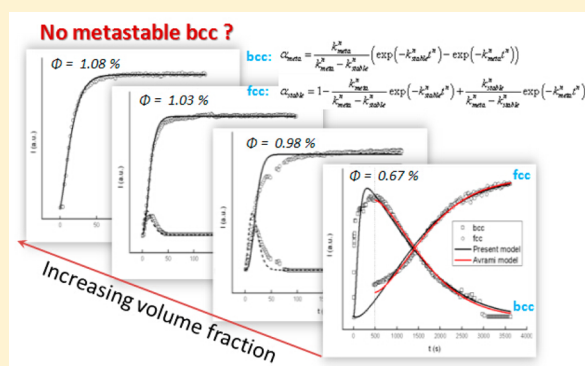
Hongwei Zhou,^{†,‡} Yanming Qin,^{†,‡,§} Shenghua Xu,^{*,†,‡} and Zhiwei Sun^{*,†,‡}

[†]Key Laboratory of Microgravity, Institute of Mechanics, Chinese Academy of Sciences, Beijing 100190, People’s Republic of China

[‡]National Microgravity Laboratory, Institute of Mechanics, Chinese Academy of Sciences, Beijing 100190, People’s Republic of China

[§]College of Chemistry, Chemical Engineering and Material Science, Shandong Normal University, Jinan 250014, People’s Republic of China

ABSTRACT: Experimental measurements of colloidal crystallization in a wide range of volume fractions of charged particles were performed to investigate the liquid–metastable–stable transition process. To fit the obtained experimental data, we developed a theoretical model to formulate the kinetics of the concurrent liquid–metastable and metastable–stable transitions. This model is well-supported by our observations. We found that when the ratio of the metastable–stable transition rate to the liquid–metastable rate is very large, the metastable state can become undetectable, although it still exists, offering a possible explanation for very few exceptions to Ostwald’s step rule.



INTRODUCTION

Colloidal crystallization has attracted a great deal of attention as a model system for mimicking the atomic or molecular counterparts, and also for assessing the validity of classical crystal growth theories.^{1–5} Understanding the nature of the structural evolution during nucleation and growth is still a fundamental and challenging issue in condensed-matter science.^{6,7} One of the major relevant topics is Ostwald’s step rule,⁸ first proposed in 1897 as an empirical rule, stating that in general it is not the most stable, but the least stable, polymorph that crystallizes first.

However, Ostwald’s step rule is not yet a universal law for two reasons. First, there are exceptions (although very few) to the rule. Second, an undisputed theoretical basis for the rule has not been formulated successfully. Over the past 100 years, various attempts were made to reach the goal, but none of them were successful. In 1978, on the basis of the mean-field treatment, Alexander and McTague⁹ published their striking result predicting that a body-centered cubic (bcc) structure should be formed first regardless of whether a more thermodynamically stable one exists, as long as the first-order nature of the transition from the liquid is not too distinct. Since then, a great deal of research attention has been devoted to finding the existence of the metastable bcc phase in various systems.^{10,11} Among these efforts, our previous studies focused more on the issues of the structural evolution in colloidal crystallization.^{12,13} We quantitatively demonstrated bcc’s formation and face-centered cubic (fcc)’s growth at the expense of metastable bcc, confirming the existence of the metastable bcc phase. However, determining how to explain the exceptions to the step rule is still an interesting issue. To explore this more

deeply, we conducted a series of experiments in an extended range of volume fractions, Φ , covering the phase behavior involved in entire liquid–metastable–stable (L–M–S) transitions. To fit the obtained experimental data, we also proposed a new theoretical model and found that the model fits the data very well.

Analyzing our experimental data with an appropriate theoretical model is critical for a better understanding of the phase transition kinetics. Dating back to 1940s, the Kolmogorov, Mehl, Johnson, and Avrami (KMJA) phenomenological model^{14–16} or the Avrami Model began to be developed for analyzing the transition kinetics of two phases. This model was broadly used in various systems, such as metallic alloys,¹⁷ a quasicrystal,¹⁸ and an ionic liquid,¹⁹ and continuous efforts have been made to improve the Avrami Model to better explain relevant phase transitions involved in some specified system.²⁰ For instance, an extension of the KMJA model was used by Wette et al.²¹ to describe the competition between the wall crystallization and bulk crystallization for a colloid system. However, all these improvements still cannot make the models properly treat two consecutive phase transformation processes. For many systems, including colloidal crystals and others, such as ice,²² amino acids,^{23,24} peptides,²⁵ and some polymers,²⁶ the metastable state is the necessary path for the transformation from the initial state to the thermodynamically stable state. In this case, the L–M transition and the M–S transition take place

Received: March 12, 2015

Revised: June 2, 2015

Published: June 16, 2015

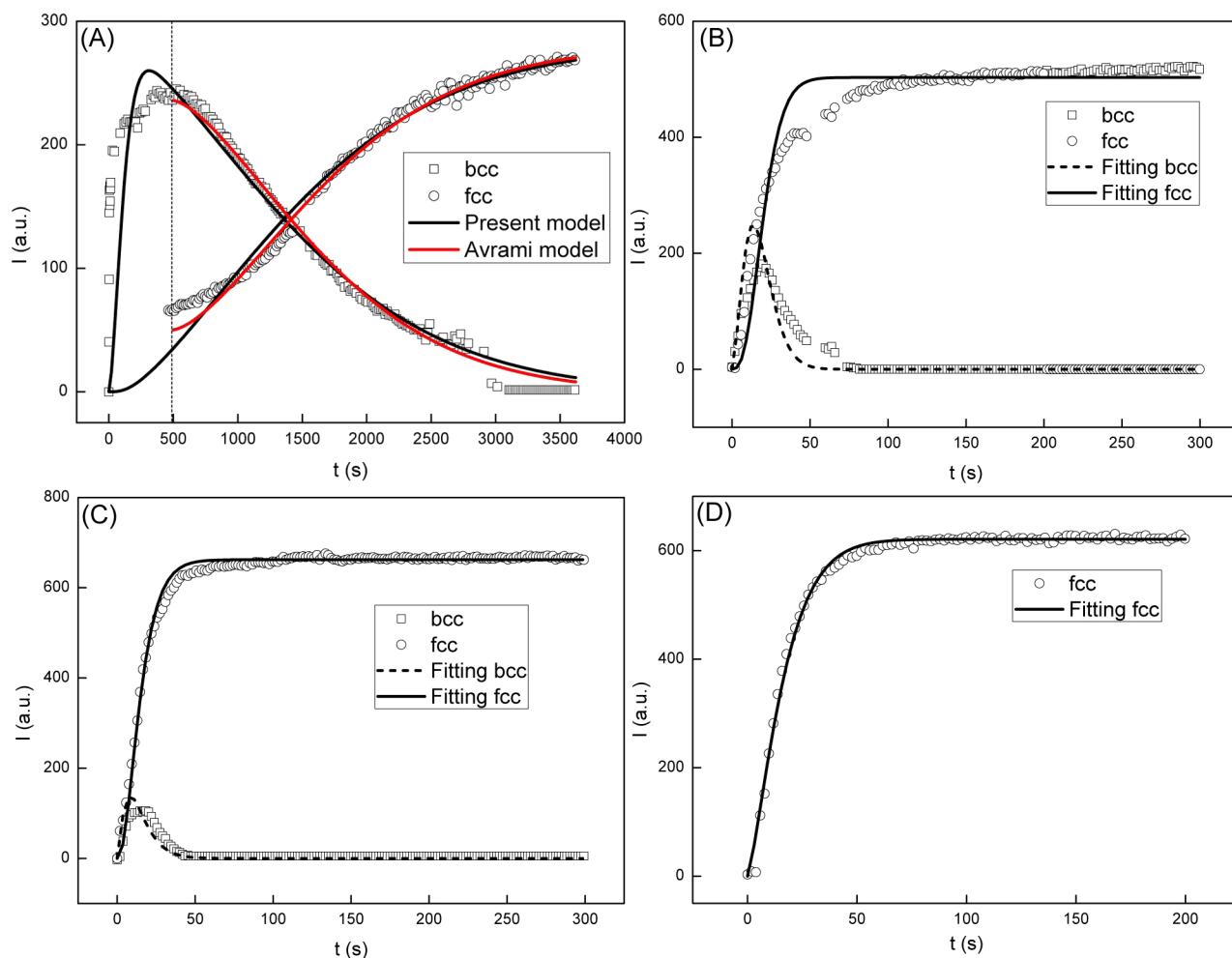


Figure 1. I - t curves of bcc and fcc with different Φ values. (A) $\Phi = 0.67\%$. The curves are fitted by the Avrami Model, as well as the model proposed in this paper. The vertical short dash line indicates the boundary of bcc growth and bcc decay. (B) $\Phi = 0.98\%$. (C) $\Phi = 1.03\%$. (D) $\Phi = 1.08\%$. The fitting results of bcc and fcc in panels B–D were obtained by using the new model proposed in this paper. Clearly, the maximal fractions of bcc decrease with an increasing Φ . No metastable bcc can be observed in panel D because it transforms into stable fcc immediately and its maximal fraction is too low to be detected.

concurrently. Namely, the formation and transformation of the metastable phase occur simultaneously, which is already beyond the validity of the Avrami Model. As we know, there is no preexisting theoretical model capable of dealing with the dynamics involved in the concurrent L–M and M–S transition.

Until now, in colloidal crystallization, only the M–S transition kinetics has been investigated by means of the Avrami Model.¹³ However, this is just a special case in which the L–M transition is so fast that the M–S transition at a later stage can ignore the existence of the initial liquid state, as discussed for other systems.²⁶ Even in such special cases, the initial stage of the L–M transition can hardly be analyzed theoretically. In this study, we aim to construct a new theoretical model using the extended volume concept that was widely accepted and used in the deduction of the Avrami Model,^{16,27} based on the experimental data collected during the colloidal crystallization process covering entire L–M–S phase transitions. As a result of our experimental and theoretical work, we provide evidence that metastable bcc forms first in the crystallization and immediately transforms to the fcc stable phase before it reaches a detectable level, offering a possible explanation for the few exceptions to Ostwald’s step rule. These findings actually coincide with Ostwald’s argument against

occasional exceptions to the rule: “...there will be cases where for a given phase transformation, a metastable phase exists, but is not observed. In those cases, one may always assume that this intermediate phase does form, but transforms immediately (into the stable phase).”⁸

■ EXPERIMENT AND THEORETICAL MODEL

Experiment. The used negatively charged polystyrene particles were synthesized by emulsion polymerization, and the mean diameter, polydispersity, and analytical charge density of the particles are 102 nm, 5.6%, and $11 \mu\text{C cm}^{-2}$, respectively. The experimental setup is the same as that in our previous papers.^{12,13} Reflection spectra recorded during the crystallization process were used to identify the crystal structure, and the peak intensities I corresponding to bcc (metastable) and fcc (stable) were used to analyze the transition kinetics.

Theoretical Model. As mentioned above, there is no preexisting theoretical model capable of dealing with the dynamics involved in the concurrent L–M and M–S transition. To solve this problem, we proposed a theoretical model based on the so-called extended volume concept^{17,27–29} for describing the transformation, which was similar to the works of KMJA.^{14–16} Specifically, the initial state volume, V_0 , the actual transformed volume, V_v and the extended volume, V_{ex_v} are related through

$$dV_t = (1 - V_t/V_0) dV_{\text{ex}_t} \quad (1)$$

This formula actually assumes that initially the full volume V_0 is of state I, and it transforms to state II for which the volume is V_t . Therefore, we can rewrite the formula to be

$$dV_t = (V_0 - V_t) dV_{\text{ex},t}/V_0 = V_1 dV_{\text{ex},t}/V_0 \quad (2)$$

where V_1 equals the volume of state I that still remains and is not yet transformed to state II. It means that the transformed volume from state I to state II is proportional to state I's residual volume V_1 and the change in extended volume $dV_{\text{ex},t}$.

As a result, now the one-step transformation (eq 2) can be extended to the two-step transformations, including liquid–metastable and metastable–stable transitions as

$$dV_{\text{stable}} = V_{\text{meta}} dV_{\text{ex,stable}}/V_0 \quad (3)$$

$$dV_{\text{meta}} = (V_{\text{liquid}} dV_{\text{ex,meta}} - V_{\text{meta}} dV_{\text{ex,stable}})/V_0 \quad (4)$$

where the subscripts stable, meta, and liquid mean the stable state, metastable state, and liquid, respectively. As in ref 28, these two formulas can be changed to

$$d\alpha_{\text{stable}} = \alpha_{\text{meta}} d\alpha_{\text{ex,stable}} \quad (5)$$

$$d\alpha_{\text{meta}} = \alpha_{\text{liquid}} d\alpha_{\text{ex,meta}} - \alpha_{\text{meta}} d\alpha_{\text{ex,stable}} \quad (6)$$

where $\alpha = V/V_0$ is the fraction of each state. According to ref 28, $\alpha_{\text{ex}} = (kt)^n$, where k is the transformation rate and n is an index related to the transformation mode. For a certain system, we can assume that the transformation modes between different states are similar, so we can get $\alpha_{\text{ex,meta}} = (k_{\text{meta}}t)^n$ and $\alpha_{\text{ex,stable}} = (k_{\text{stable}}t)^n$, where k_{meta} and k_{stable} represent the rates for liquid–metastable and metastable–stable transformations, respectively. In eq 6, $\alpha_{\text{liquid}} = 1 - \alpha_{\text{meta}} - \alpha_{\text{stable}}$. Then we have

$$d\alpha_{\text{stable}}/dt^n = k_{\text{stable}}^n \alpha_{\text{meta}} \quad (7)$$

$$d\alpha_{\text{meta}}/dt^n = k_{\text{meta}}^n (1 - \alpha_{\text{meta}} - \alpha_{\text{stable}}) - k_{\text{stable}}^n \alpha_{\text{meta}} \quad (8)$$

With boundary conditions $\alpha_{\text{meta}}(t=0) = 0$, $\alpha_{\text{stable}}(t=0) = 0$, $\alpha_{\text{meta}}(t=\infty) = 0$, and $\alpha_{\text{stable}}(t=\infty) = 1$, the solution for eqs 7 and 8 is

$$\alpha_{\text{meta}} = \frac{k_{\text{meta}}^n [\exp(-k_{\text{stable}}^n t^n) - \exp(-k_{\text{meta}}^n t^n)]}{(k_{\text{meta}}^n - k_{\text{stable}}^n)} \quad (9)$$

$$\alpha_{\text{stable}} = 1 - \frac{k_{\text{meta}}^n \exp(-k_{\text{stable}}^n t^n) / (k_{\text{meta}}^n - k_{\text{stable}}^n) + k_{\text{stable}}^n \exp(-k_{\text{meta}}^n t^n) / (k_{\text{meta}}^n - k_{\text{stable}}^n)}{1} \quad (10)$$

It is noticed that when $k_{\text{meta}} = k_{\text{stable}} = k$, the solution should be

$$\alpha_{\text{meta}} = k^n t^n \exp(-k^n t^n) \quad (11)$$

$$\alpha_{\text{stable}} = 1 - \exp(-k^n t^n) - k^n t^n \exp(-k^n t^n) \quad (12)$$

but the results of eqs 9 and 10 converge to this equation when k_{meta} is close to k_{stable} , so that we can still use eqs 9 and 10 in this study.

RESULTS AND DISCUSSION

Panels A–D of Figure 1 are plots of $I-t$ curves of bcc and fcc with increasing Φ values of 0.67, 0.98, 1.03, and 1.08%, respectively. An obvious tendency is that the peak intensity of metastable bcc decreases with an increasing Φ until bcc totally disappears.

The curve for a low Φ (0.67%) is similar to that from a previous study.¹³ The peak intensity of metastable bcc increases rapidly to its maximum and then decreases slowly, accompanied by an increase in that of fcc. In general, the $I-t$ curve of bcc can be approximately divided into two stages: bcc growth and bcc decay. For the second stage, the $I-t$ curve could be fitted by the Avrami Model. However, because the Avrami Model can be applied to only two-phase transformations, it cannot be used to

analyze the liquid–bcc transition at the same time. Therefore, the kinetics of metastable bcc growth stage cannot be concurrently investigated in the frame of the Avrami Model.

The results for Φ values of 0.98 and 1.03% in panels B and C of Figure 1, respectively, show that with the increase in Φ , the crystallization process can no longer be distinctly divided into bcc growth and bcc decay periods. fcc may grow even faster than bcc from the beginning of the crystallization, and the maximal intensity of the metastable bcc state becomes much smaller than that of the fcc state, which are quite different from Figure 1A. These experimental results indicate liquid–bcc and bcc–fcc transitions take place concurrently, and the two transition processes can strongly influence each other. All of these situations cannot be treated by the Avrami Model.

The result with Φ increased to 1.08% is shown in Figure 1D. In this case, we simply have no way to find metastable bcc structure so that there is only the $I-t$ curve of fcc. This result looks like another exception to Ostwald's step rule. However, from the tendency that the peak intensity of metastable bcc decreases with an increasing Φ , it is reasonable to conclude that there still exists a metastable bcc state, but its peak intensity is too low to be detected.

The experimental $I-t$ curves can be fitted by our theoretical model (eqs 9 and 10). Considering the measured I is proportional to crystal size, a normalized parameter C was used to connect I with the fraction of state α so that $I_{\text{bcc}} = C\alpha_{\text{bcc}}$ and $I_{\text{fcc}} = C\alpha_{\text{fcc}}$ in the fitting.

For a Φ value of 0.67%, the fitted curves using our model are shown in Figure 1A. Obviously, in the bcc decay period, the fitted curves using our model are very close to those of the Avrami Model. Moreover, our model can also fit the curve in the metastable bcc growth period, which is already beyond the capability of the Avrami Model. The fitting parameters, n and k^n , obtained from the Avrami Model and the present model are 1.52 and 1.54, respectively, and 1.5×10^{-5} and 1.1×10^{-5} , respectively, as listed in Table 1. Our results show that $k_{\text{stable}}^n /$

Table 1. Parameters Obtained from Curve Fitting of bcc and fcc

Φ	n	k_{meta}^n	k_{stable}^n	$k_{\text{stable}}^n / k_{\text{meta}}^n$
0.67% Avrami	1.52	–	1.5×10^{-5}	–
0.67%	1.54	5.9×10^{-4}	1.1×10^{-5}	0.02
0.98%	1.55	0.024	0.012	0.50
1.03%	1.24	0.042	0.111	2.64
1.08%	1.31	0.023	∞	∞

$k_{\text{meta}}^n = 0.02$, which is much smaller than 1. For this condition ($k_{\text{stable}}^n / k_{\text{meta}}^n \ll 1$), the term $\exp(-k_{\text{meta}}^n t^n)$ in eqs 9 and 10 can be neglected, so that the two equations can be reduced to the Avrami Model. This theoretical analysis could give an explicit explanation why the Avrami Model can be used for the bcc–fcc transition in previous studies^{13,26} in which the liquid–metastable transition is very fast and the relevant metastable–stable transition is slow.

For Φ values of 0.98 and 1.03%, our model can still fit the $I_{\text{bcc}}-t$ and $I_{\text{fcc}}-t$ curves quite well (see Figure 1B,C), although the Avrami Model was no longer applicable. The obtained $k_{\text{stable}}^n / k_{\text{meta}}^n$ is 0.50 for 0.98% and 2.64 for 1.03%, which means the metastable–stable transition rate becomes comparable to or even larger than the liquid–metastable transition rate, and that is the key factor resulting in the difference between panels B and C of Figure 1 and panel A of Figure 1.

For a Φ value of 1.08%, metastable bcc is no longer observable, and the theoretical model can also be used to analyze the crystallization process (see Figure 1D). The discussion given above has shown $k_{\text{stable}}^n/k_{\text{meta}}^n$ increased rapidly with volume fraction Φ . From this tendency, we can conclude that $k_{\text{stable}}^n/k_{\text{meta}}^n$ reaches a quite large value for 1.08%. Therefore, $k_{\text{meta}}^n/(k_{\text{meta}}^n - k_{\text{stable}}^n)$ becomes close to 0; eq 9 becomes $\alpha_{\text{meta}} \approx 0$, and eq 10 becomes $\alpha_{\text{stable}} \approx \alpha_{\text{stable}} + \alpha_{\text{meta}} = 1 - \exp(-k_{\text{meta}}^n t^n)$. For this condition, the $I-t$ curve of the stable fcc state fitted by eq 10 was also consistent with the experimental result. The obtained fitting parameters, n and k_{meta}^n , are 1.31 and 0.023, respectively. It should be noted that the value of k_{stable}^n is too large to be determined with accuracy in this case.

Obviously, results of the experiments indicate that $k_{\text{stable}}^n/k_{\text{meta}}^n$ has great influence on the liquid–metastable–stable transition, especially on $\alpha_{\text{meta_max}}/\alpha_{\text{stable_max}}$ (the ratio of the maximal fraction α of metastable and stable state). To better understand the influence of $k_{\text{stable}}^n/k_{\text{meta}}^n$ on $\alpha_{\text{meta_max}}/\alpha_{\text{stable_max}}$, we deduced the expression of $\alpha_{\text{meta_max}}/\alpha_{\text{stable_max}}$ from eqs 9 and 10, which is

$$\frac{\alpha_{\text{meta_max}}}{\alpha_{\text{stable_max}}} = R^{R/1-R} \quad (13)$$

where $R = k_{\text{stable}}^n/k_{\text{meta}}^n$. When $R \rightarrow 0$, the limit of eq 13 is 1, which is the case when the Avrami Model is applicable as in Figure 1A. When $R \rightarrow \infty$, the limit of eq 13 is 0, so that $\alpha_{\text{meta_max}}$ could be too small to be observed. This is the reason why there are circumstances in which no metastable state can be detected (Figure 1D). It should be noticed that the limit value for $R = 1$ is $1/e$, which is also the value of $\alpha_{\text{meta_max}}/\alpha_{\text{stable_max}}$ for eqs 11 and 12. This is further proof that our theoretical model in eqs 9 and 10 converges to the solution when k_{meta}^n is close to k_{stable}^n , as mentioned above. In Figure 2, we can see that $\alpha_{\text{meta_max}}/\alpha_{\text{stable_max}}$ decreases with an increasing $k_{\text{stable}}^n/k_{\text{meta}}^n$, so the peak of the metastable phase drops to zero quickly.

Most methods for determining the crystal structure rely on the Bragg peak resulting from constructive interference of light scattering from the crystalline sample and need a minimal crystallite size; namely, there is a detection limit for sample size. From Table 1, we can see that the liquid–metastable

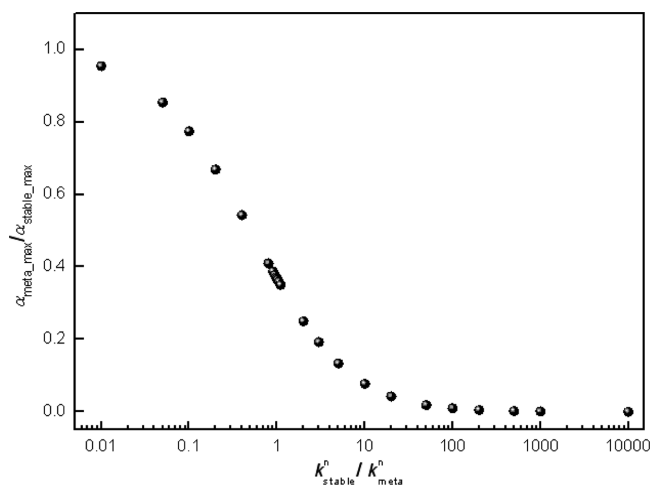


Figure 2. Calculated relationship between $\alpha_{\text{meta_max}}/\alpha_{\text{stable_max}}$ and $k_{\text{stable}}^n/k_{\text{meta}}^n$.

transformation rates for Φ values of 0.98, 1.03, and 1.08% are 0.024, 0.042, and 0.023, respectively. That is, the magnitude of the rates of transformation (k_{meta}^n) from liquid to bcc is basically unchanged (except for $\Phi = 0.67\%$), implying the metastable bcc should form with approximately the same rate, even though it is not detectable. On the other hand, the rates of transformation from bcc to fcc increase rapidly with an increasing Φ . Therefore, the real reason for bcc being undetectable when $\Phi = 1.08\%$ is that the rate of transformation (k_{stable}^n) from bcc to fcc becomes too large. In this case, the metastable bcc phase (or local structures) has already transformed to fcc before it reaches the detection limit, and therefore, one will not be able to detect it.

This situation is rather analogous to a rabbit eating grass: grass grows from soil, and a rabbit grows by eating grass. If the eating rate is much higher than the grass growth rate, the grass will be too little to be seen, but it does not mean that grass never grows. Therefore, our findings provide a possible explanation for the exceptions to Ostwald's step rule. Here, it would be interesting to recall Ostwald's statement: "it is easy to formulate such a hypothesis, yet not always possible to prove it with existing techniques. However, in many of these cases it will be possible to find the appropriate means to slow down the reaction (i.e. the phase transformation) to enable the observation of the intermediate phase." So Ostwald thought the reason for some exceptions is that the existing technique may not be fast enough to detect the metastable phase. However, our findings show that the key problem is not the liquid–metastable transformation rate itself, as assumed by Ostwald; instead, the determinative factor is the ratio of the metastable–stable transition rate to the liquid–metastable rate ($k_{\text{stable}}^n/k_{\text{meta}}^n$). In fact, currently our highest sampling rate of identifying the crystal structure has been improved greatly from the previous value of 4 times/s^{12,13} to 100 times/s. Namely, now we need only 0.01 ms to finish one measurement of the crystal type. Even with a technique that is so fast, we still could not find metastable bcc in the case of $\Phi = 1.08\%$, demonstrating that slowing the reaction (or increasing the measuring rate) cannot solve the problem of making the invisible metastable phase visible. The key problem should be how rapidly the bcc–fcc transition ("reaction") proceeds compared to the liquid–bcc one.

Alternatively, what we discussed above can be easily understood by considering the free energy variations associated with the formation of the nucleus. According to the Arrhenius equation, $\Omega = A \exp(-\Delta G/k_B T)$, where Ω is the nucleation rate, ΔG is the kinetic barrier from the initial state to the final state, A is a pre-exponential factor, and $k_B T$ is the thermal energy. Considering the crystallization transition from the parent liquid (or melt) state to the globally stable daughter solid phase, we use ΔG_{l-s} to denote the relevant kinetic barrier. In our case, the parent phase is the liquid phase and the daughter and metastable phases are fcc and bcc, respectively. A phase transition requires passage over a free energy barrier. Panels A–C of Figure 1 doubtlessly demonstrate the evidence of the presence of the metastable bcc phase. Now we can divide the liquid–fcc nucleation process into two steps: liquid–bcc and bcc–fcc. The reason for the presence of the metastable phase is that its presence can provide an alternative, lower-energy nucleation–growth pathway. That is, the barrier of $\Delta G_{l-bcc} + \Delta G_{bcc-fcc}$ should be lower than those associated with all other possible pathways. The bcc metastable phases in Figure 1A–C are observable because the rates of transition

from bcc to fcc are either less than or comparable to the corresponding rates from liquid to bcc. From Figure 1A–D, the heights of the barriers ($\Delta G_{\text{bcc-fcc}}$) or the so-called critical nucleus sizes (CNZ) are getting smaller so that bcc phase becomes more and more difficult to observe. For Figure 1D, we even cannot say whether bcc still exists as a phase. If CNZ are so small that the sizes of formed bcc clusters are below the detection limit, we will not be able to observe them. Actually, when CNZ are reduced to less than one growth unit, whenever bcc structure forms, it is transformed into fcc structure immediately. In this case, we suppose the barrier for the bcc–fcc transition ($\Delta G_{\text{bcc-fcc}}$) vanishes and the formed bcc phase becomes unstable. In other words, the intermediate bcc structure still forms first because of its lower barrier ($\Delta G_{\text{l-bcc}}$) but is unstable and decays to fcc structure immediately, which is spinodal decomposition. $\Delta G_{\text{bcc-fcc}} \approx 0$ leads to a very large bcc–fcc transition rate, and the total liquid–fcc transition rate is actually controlled by the liquid–bcc transition. The precursors of nucleation in colloidal crystallization were confirmed in a microscopic observation by means of laser scanning confocal microscopy.⁶ Very recent simulations of the homogeneous liquid–fcc nucleation of charged colloids by K. Kratzer et al. also show that the liquid–fcc transition involves two stages of the liquid–bcc and bcc–hcp/fcc transitions.³⁰ As they specially addressed, “according to Ostwald, the phase which is closest to the initial state in free energy is nucleated first, which doesn’t have to be the truly stable phase. In addition, Stranski and Totomanow found that the phase with the lowest free energy barrier is nucleated first...”³⁰

The argument described above is also nicely supported by the recent study of M. Santra et al. based on the density functional theory.³¹ Their study shows “nucleation of the solid phase from the melt may be facilitated by the metastable phase because the latter can “wet” the interface between the parent and the daughter phases, even though there may be no signature of the existence of metastable phase in the thermodynamic properties of the parent liquid and the stable solid phase.”³¹ They find that “the nucleation free energy barrier can decrease significantly in the presence of wetting.”³¹ Apparently, the existence of metastable phase lowers the interface tension between the parent and the daughter phases and therefore reduces the nucleation barrier or the critical nucleus size.

CONCLUSIONS

In summary, Φ -dependent colloidal crystallization experiments were conducted to investigate the uncut concurrent liquid–metastable–stable transition kinetics. We found liquid–metastable and metastable–stable transitions may have important mutual influences on their kinetics, which cannot be effectively treated by a preexisting theoretical model, and a theoretical model was developed to understand the concurrent liquid–metastable and metastable–stable transition kinetics. The model not only can quantitatively explain the experimental results but also covers the Avrami Model that can be applied only to the transformation of two phases. This new model unifies phase transition kinetics regardless of whether Ostwald’s step rule is obeyed. Therefore, it would supposedly be applicable to the crystallization of a variety of systems with a metastable state, and in principle, it can be extended to treat the concurrent phase transition kinetics with multiple metastable states.

In addition, our results show that the liquid–metastable–stable transition may be greatly influenced by the ratio of two rates, $k_{\text{stable}}^n/k_{\text{meta}}^n$, which means the absolute value of k_{stable}^n and k_{meta}^n is not the key factor but their ratio is. When $k_{\text{stable}}^n/k_{\text{meta}}^n$ is very large, the metastable state becomes too little to be detected because its maximal fraction during crystallization is too low.

The case in which $\Phi = 1.08\%$ does show that there is no metastable bcc observable while the fcc is the stable phase. Can we conclude that it is another exception to the step rule? It is probably not, because, as discussed above, whenever bcc forms, it is transformed to fcc immediately, making the amount of bcc left below the detection limit or it is simply unstable and decays to the stable state immediately. In any cases, on the basis of our experiment and analysis, this study raises suspicions about whether the reported exceptions to Ostwald’s step rule are all real exceptions.

As a separate note, our observation confirms the presence of the metastable phase, which is bcc. In practice, however, the number of the metastable phase involved in crystallization may be more than one and may not necessarily be bcc.

AUTHOR INFORMATION

Corresponding Authors

*E-mail: xush@imech.ac.cn.

*E-mail: sunzw@imech.ac.cn.

Notes

The authors declare no competing financial interest.

ACKNOWLEDGMENTS

This work is supported by the National Natural Science Foundation of China (11302226, 11172302, and 11032011).

REFERENCES

- (1) Auer, S.; Frenkel, D. Prediction of absolute crystal-nucleation rate in hard-sphere colloids. *Nature* **2001**, *409*, 1020–1023.
- (2) Schall, P.; Cohen, I.; Weitz, D. A.; Spaepen, F. Visualizing dislocation nucleation by indenting colloidal crystals. *Nature* **2006**, *440*, 319–323.
- (3) Zhang, T. H.; Liu, X. Y. Experimental modelling of single-particle dynamic processes in crystallization by controlled colloidal assembly. *Chem. Soc. Rev.* **2014**, *43*, 2324–2347.
- (4) Wette, P.; Klassen, I.; Holland-Moritz, D.; Palberg, T.; Roth, S. V.; Herlach, D. M. Colloids as model systems for liquid undercooled metals. *Phys. Rev. E* **2009**, *79*, 010501.
- (5) Aastuen, D. J. W.; Clark, N. A.; Cotter, L. K.; Ackerson, B. J. Nucleation and Growth of Colloidal Crystals. *Phys. Rev. Lett.* **1986**, *57*, 1733–1736.
- (6) Tan, P.; Xu, N.; Xu, L. Visualizing kinetic pathways of homogeneous nucleation in colloidal crystallization. *Nat. Phys.* **2014**, *10*, 73–79.
- (7) Peng, Y.; Wang, F.; Wang, Z.; Alsayed, A. M.; Zhang, Z.; Yodh, A. G.; Han, Y. Two-step nucleation mechanism in solid–solid phase transitions. *Nat. Mater.* **2015**, *14*, 101–108.
- (8) Ostwald, W. Z. *Phys. Chem.* **1897**, *22*, 289.
- (9) Alexander, S.; McTague, J. Should All Crystals Be bcc? Landau Theory of Solidification and Crystal Nucleation. *Phys. Rev. Lett.* **1978**, *41*, 702–705.
- (10) Notthoff, C.; Feuerbacher, B.; Franz, H.; Herlach, D. M.; Holland-Moritz, D. Direct Determination of Metastable Phase Diagram by Synchrotron Radiation Experiments on Undercooled Metallic Melts. *Phys. Rev. Lett.* **2001**, *86*, 1038–1041.
- (11) Bang, J.; Lodge, T. P. Long-Lived Metastable bcc Phase during Ordering of Micelles. *Phys. Rev. Lett.* **2004**, *93*, 245701.

- (12) Xu, S.; Zhou, H.; Sun, Z.; Xie, J. Formation of an fcc phase through a bcc metastable state in crystallization of charged colloidal particles. *Phys. Rev. E* **2010**, *82*, 010401.
- (13) Zhou, H.; Xu, S.; Sun, Z.; Du, X.; Liu, L. Kinetics Study of Crystallization with the Disorder–bcc–fcc Phase Transition of Charged Colloidal Dispersions. *Langmuir* **2011**, *27*, 7439–7445.
- (14) Kolmogorov, A. N. *Bulletin of the Academy of Sciences of USSR, Physical Series 1* **1937**, 355.
- (15) Johnson, W. A.; Mehl, R. F. Reaction kinetics in processes of nucleation and growth. *Trans. Am. Inst. Min., Metall. Pet. Eng.* **1939**, *135*, 416–442.
- (16) (a) Avrami, M. Kinetics of Phase Change. I. General Theory. *J. Chem. Phys.* **1939**, *7*, 1103–1112. (b) Avrami, M. Kinetics of Phase Change. II Transformation-Time Relations for Random Distribution of Nuclei. *J. Chem. Phys.* **1940**, *8*, 212–224. (c) Avrami, M. Granulation, Phase Change, and Microstructure Kinetics of Phase Change. III. *J. Chem. Phys.* **1941**, *9*, 177–184.
- (17) Christian, J. W. *The Theory of Transformation in Metals and Alloys*, 2nd ed.; Pergamon Press: Oxford, U.K., 1975; Part 1.
- (18) Jiang, J. Z.; Zhuang, Y. X.; Rasmussen, H.; Saida, J.; Inoue, A. Formation of quasicrystals and amorphous-to-quasicrystalline phase transformation kinetics in $Zr_{65}Al_{7.5}Ni_{10}Cu_{7.5}Ag_{10}$ metallic glass under pressure. *Phys. Rev. B* **2001**, *64*, 094208.
- (19) Pas, S. J.; Dargusch, M. S.; MacFarlane, D. R. Crystallisation kinetics of some archetypal ionic liquids: Isothermal and non-isothermal determination of the Avrami exponent. *Phys. Chem. Chem. Phys.* **2011**, *13*, 12033–12040.
- (20) Narine, S. S.; Humphrey, K. L.; Bouzidi, L. Modification of the Avrami Model for Application to the Kinetics of the Melt Crystallization of Lipids. *J. Am. Oil Chem. Soc.* **2006**, *83*, 913–921.
- (21) Wette, P.; Schope, H. J.; Palberg, T. Microscopic investigations of homogeneous nucleation in charged sphere suspensions. *J. Chem. Phys.* **2005**, *123*, 174902.
- (22) Russo, J.; Romano, F.; Tanaka, H. New metastable form of ice and its role in the homogeneous crystallization of water. *Nat. Mater.* **2014**, *13*, 733–739.
- (23) Hall, V. J.; Simpson, G. J. Direct Observation of Transient Ostwald Crystallization Ordering from Racemic Serine Solutions. *J. Am. Chem. Soc.* **2010**, *132*, 13598–13599.
- (24) Chowdhury, A. U.; Dettmar, C. M.; Sullivan, S. Z.; Zhang, S.; Jacobs, K. T.; Kissick, D. J.; Maltais, T.; Hedderich, H. G.; Bishop, P. A.; Simpson, G. J. Kinetic Trapping of Metastable Amino Acid Polymorphs. *J. Am. Chem. Soc.* **2014**, *136*, 2404–2412.
- (25) Liang, C.; Ni, R.; Smith, J. E.; Childers, W. S.; Mehta, A. K.; Lynn, D. G. Kinetic Intermediates in Amyloid Assembly. *J. Am. Chem. Soc.* **2014**, *136*, 15146–15149.
- (26) Liu, Y. S.; Nie, H. F.; Bansil, R.; Steinhart, M.; Bang, J.; Lodge, T. P. Kinetics of disorder-to-fcc phase transition via an intermediate bcc state. *Phys. Rev. E* **2006**, *73*, 061803.
- (27) Piorkowska, E.; Galeski, A.; Haudin, J. M. Critical assessment of overall crystallization kinetics theories and predictions. *Prog. Polym. Sci.* **2006**, *31*, 549–575.
- (28) Starink, M. J. Kinetic equations for diffusion-controlled precipitation reactions. *J. Mater. Sci.* **1997**, *32*, 4061–4070.
- (29) Erukhimovitch, V.; Baram, J. Crystallization kinetics. *Phys. Rev. B* **1994**, *50*, 5854–5856.
- (30) Kratzer, K.; Arnold, A. Two-stage crystallization of charged colloids under low supersaturation conditions. *Soft Matter* **2015**, *11*, 2174–2182.
- (31) Santra, M.; Singh, R. S.; Bagchi, B. Nucleation of a Stable Solid from Melt in the Presence of Multiple Metastable Intermediate Phases: Wetting, Ostwald's Step Rule, and Vanishing Polymorphs. *J. Phys. Chem. B* **2013**, *117*, 13154–13163.